Review

Transition Metal Compounds Towards Holography

Volker Dieckmann, Sebastian Eicke, Kristin Springfeld and Mirco Imlau ⋆

Department of Physics, University of Osnabrück, Barbarastraße 7, Osnabrück 49076, Germany;
E-Mails: vdieckma@uos.de (V.D.); seicke@uos.de (S.E.); kspringf@uos.de (K.S.)

⋆ Author to whom correspondence should be addressed; E-Mail: mimlau@uos.de;
Tel.: +49-0541-969-2654; Fax: +49-0541-969-3510.

Abstract: We have successfully proposed the application of transition metal compounds in holographic recording media. Such compounds feature an ultra-fast light-induced linkage isomerization of the transition-metal–ligand bond with switching times in the sub-picosecond regime and lifetimes from microseconds up to hours at room temperature. This article highlights the photofunctionality of two of the most promising transition metal compounds and the photophysical mechanisms that are underlying the hologram recording. We present the latest progress with respect to the key measures of holographic media assembled from transition metal compounds, the molecular embedding in a dielectric matrix and their impressive potential for modern holographic applications.

Keywords: transition metal compounds; holographic recording materials; nonlinear optics; applications

Classification: PACS 42.40.-i, 42.40.My, 42.65.-k, 42.70.Ln

1. Introduction

It has been a visionary nanoscopic approach to apply functional transition metal compounds for the development of advanced materials for modern holography [1–3]: light-induced linkage isomerization on a molecular level alters the macroscopic susceptibility of the medium [4,5], thus allowing for hologram recording with a spatial resolution up to one line per nanometer unknown, so far. Already in 1996,

we succeeded in the recording of elementary volume holograms in single crystals of photofunctional compounds of $[Fe(CN)_5NO]^{2-}$ (sodium nitroprusside, SNP) showing tremendous amplitudes of the optically induced refractive-index change of more than 10^{-2} via NO isomerization. By far more exciting—from the point of view of applications—was the successful demonstration of a full optical write-read-erasure cycle that has become possible due to the optical reversibility of the linkage isomerization in these compounds (see Figure 1a) [3]. Even a series of phase holograms could be recorded within the same molecular 3D-array by means of angular multiplexing (see Figure 1b) [3].

Figure 1. (**a**) Write-read-erasure cycle of a hologram recorded in a single crystal of $Na_2[Fe(CN)_5NO]\cdot 2H_2O$ (wavelengths $\lambda_{record,read}$ = 514.5 nm, intensities $I_{reference}$ = I_{signal} = (100 ± 5) mW cm^{-2}). Inset: Picture of a b-cut SNP single crystal (thickness $d = 340\,\mu$m, sample by Th. Woike, TU Dresden); (**b**) Multiplexed recording of seven holograms within the same volume element of a SNP single crystal. The holograms were recorded sequentially by angular rotation of the medium by $5°$. All data taken from Reference [3].
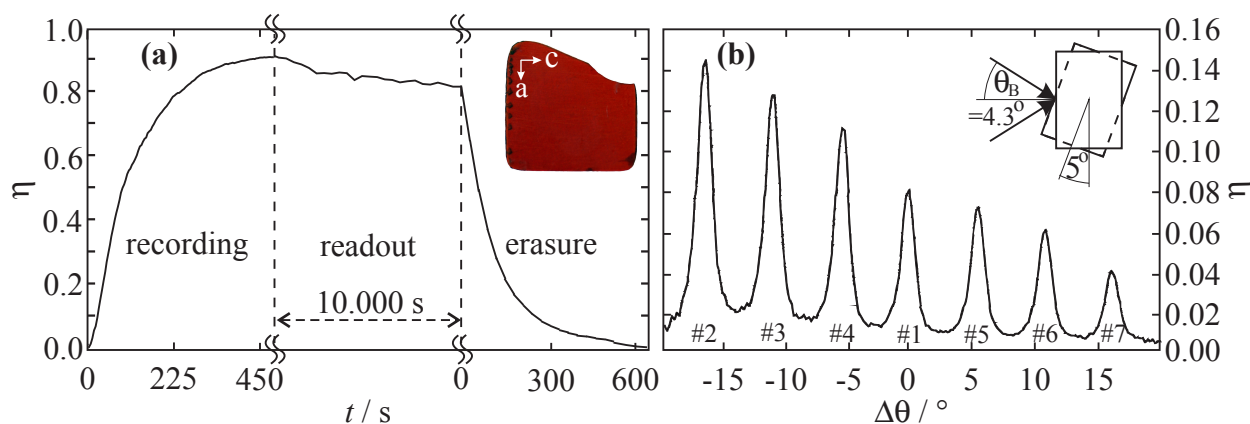
Based on these results, hologram media assembled from photofunctional transition metal compounds were primarily intended as bulk media for optical storage of large data streams by means of holography [1,4,6]. It is because of the impressive storage density in the order of TBit cm^{-3}, the possibility to fabricate amply dimensioned media at low cost and the promising hologram stability with thermally activated decay times of more than 10^{15} s at temperatures of liquid nitrogen [7]. At room temperature, the photofunctionality of NP-compounds features thermal relaxation times in the order of milli- and microseconds [8], while the time scale of the optically triggered isomerization process is reported in the sub-picosecond regime [9]. Applied to holography, real-time dynamic holography and self-erasure at kilohertz frequencies becomes feasible, allowing for a variety of fascinating applications. In the area of information and communication technologies, this includes real-time/real-3D holographic displays as well as ultrafast switches for photonic networks [10–13].

The relation between the photophysical properties and features of transition metal compounds with modern holographic applications is highlighted in more detail in Table 1. Exemplarily, the device specifications relevant for the applications are given for dynamical Bragg filters, phase conjugate mirrors, holographic data storage system and holographic displays and are translated to the corresponding transition metal compound features.

Table 1. Relation between the photophysical properties and features of transition metal compounds with modern holographic applications by taking into account the relevant device specifications.

Holographic application	Key macroscopic specification	Compound feature
Dynamical Bragg filter	GHz-THz-switching frequencies	(ultra-)fast linkage isomerization
		optically reversible isomerization *or* short lifetimes of the isomers
	wavelength resolution $< 0.5\,\mathrm{nm}$	pronounced photorefractivity
	low losses	low absorption
	sample dimensions $\sim 1\,\mathrm{cm}^3$	suited for embedding in bulk dielectric media
Phase conjugate mirrors	self-adjusting	optically reversible isomerization
	low cycle fatigue	isomerization without aging/fatigue
	sample dimensions $\sim 1\,\mathrm{cm}^3$	suited for embedding in bulk dielectric media
Holographic data storage	(ultra-)fast write-read-erasure cycle	(ultra-)fast linkage isomerization
		optically reversible isomerization
	ready for multiplexing	pronounced photorefractivity
	long data lifetime	high thermal stability of isomers
	low cycle fatigue	isomerization without aging/fatigue
	sample dimensions $\sim 10\,\mathrm{cm}^3$	suited for embedding in bulk dielectric media
Real-time, real-3D holographic displays	spatial resolution ($< 100\,\mathrm{l}/\mu\mathrm{m}$)	small molecules
	200 Hz refresh rate	(ultra-)fast linkage isomerization
		optically reversible isomerization *or* short lifetimes of the isomers
	low cycle fatigue	isomerization without aging/fatigue
	high contrast	pronounced photorefractivity and photochromism

Table 1. *Cont* .

Holographic application	Key macroscopic specification	Compound feature
	full color (RGB) display	photosensitivity in the blue, green and red spectral range
	sample dimensions $\sim 1\,\mathrm{m}^2$	suited for embedding in dielectric thick films

Obviously, rather different and contrary compound features are required depending on the type of holographic application. This fostered the synthesis of a broad spectrum of appropriate, different transition metal compounds over the last decade [14]. Also, the possibilities for tuning the molecular features by ligand substitution or substitution of the central metal atom have been widely addressed within this context [15,16]. At the same time, the embedding of transition metal compounds into bulk dielectric media and films turned out as an important next step towards the realization of visionary applications [17,18].

Beyond the molecular point of view, the development of molecular-based holographic media enforces to specify the key measures that have been widely accepted for holographic recording materials. The volume density of molecules and their absorption cross section limit the *hologram modulation depth*, *i.e.*, the maximum amplitude of photochromic and/or photorefractive response. The quantum yield for the light-induced linkage isomerization is responsible for the *hologram sensitivity* given by the amount of light exposure required for reaching the maximum modulation depth. The photon energy necessary to trigger the photoisomerization affects the *spectral hologram sensitivity*. The potential barrier between isomerization state and ground state defines the *hologram lifetime*. The molecular dimensions and concentration limit the *spatial resolution* that is far beyond the needs for the mentioned applications taking the atomic scale into account. Finally, the interplay between molecular compound and dielectric environment must be taken into account for the synthesis of *large scale thick media* while the selection rule for ligands is restricted in the view of a non-toxic, low-cost medium that can be recycled.

The task of this article is to summarize the state of the art of photofunctional transition metal compounds in the view of holographic media development for modern holographic applications. We present the two most promising classes of transition metal compounds, *i.e.*, the nitroprusside and sulfoxide compounds. They feature (ultra-)fast light-induced linkage isomerization of the NO- and SO-ligand, respectively, with promising quantum yield and appropriate energy landscape that can be adjusted by metal and/or ligand substitution. Furthermore, hologram media can be synthesized on a large scale, at low cost and without toxic ligands.

2. Photophysical Properties of Transition Metal Compounds

The key photofunctionality of transition metal compounds that are of interest for hologram media development is a linkage isomerization process: Triggered by a metal-to-ligand charge-transfer (MLCT) transition, an ultrafast unimolecular structural alteration is performed within sub-nano- or

picoseconds [9,19]. This process is accompanied with pronounced modifications of the electronic structure of the molecule yielding thereby tremendous photochromic and photorefractive responses that are intended for efficient hologram recording [3,20].

The photofunctionality and its optical and temporal features can be related to the electronic and molecular structure within the principle scheme depicted in Figure 2. Starting from the electronic ground state GS, an antibonding state GS* can be addressed by optical means via a charge transfer from the central metal to a molecular orbital located at one of its ligands [21]. It is a Franck–Condon excitation with a photon energy $E_{\text{ph}}^{\text{MLCT}}$. The excited state GS* relaxes within picoseconds to an energetic minimum in the excited state energy landscape, usually with triplet multiplicity [22,23]. Changes in the molecular structure driven by this electronic relaxation are accounted for by propagation along the reaction coordinate. As a result, a new electronic ground state is formed, designated by MS, and allows for electronic relaxation from the excited state energy landscape to MS. The electronic state MS is metastable due to its energetic level well above GS and is separated by a potential barrier E_{A}, typically with height in the order of a few 100 meV. Furthermore, photons with energy $E_{\text{ph}}^{\text{MS}} < E_{\text{ph}}^{\text{MLCT}}$ may be absorbed.

Figure 2. Scheme of a light-induced linkage isomerization in a transition metal compound. The reaction is triggered by a MLCT transition from GS to the excited GS* with subsequent isomerization to a metastable ground state MS. Optically induced reaction from MS to GS can be possible depending on the energetic structure of the compound.
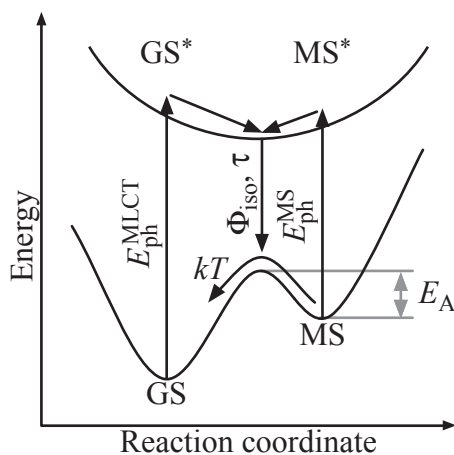

The isomerization process thereby can be probed by optical means via photon absorption with energy $E_{\text{ph}}^{\text{MLCT}}$ and $E_{\text{ph}}^{\text{MS}}$. Its quantum efficiency Θ_{iso} is determined by the MLCT transition probability and probability for relaxation from the excited state energy landscape into MS (instead of GS). The isomerization process duration $\tau_{\text{GS}\to\text{MS}}$ is mainly determined by the electronic relaxation GS$^\star \to$ MS*, thus commonly in the sub-picosecond regime. We note that an optically induced transfer MS $\to$ GS may principally be possible by excitation to MS* besides the thermally activated decay, as well. Such optical backswitching particularly is of interest for a variety of holographic applications, as it allows for the development of a fully addressable holographic medium (write-read-erasure cycle).

In the view of the presented principle scheme, we will now introduce the photofunctionality of two outstanding classes of transition metal compounds, nitroprussides and sulfoxides, in more detail.

Although we must consider a more complex, three-dimensional energy landscape including three ground states with different reaction coordinates, the principle photofunctionality of Figure 2 is preserved.

The structural ground state of nitroprusside compounds $[ML_5NO]^{m\pm}$, with M being the central transition metal, L ligands and $m\pm$ the overall charge, is depicted in Figure 3 with $[Fe(CN)_5)NO]^{2-}$ as an example. Its photofunctionality is located at the Fe-N-O bond. Initiated by a MLCT transition from the central Fe atom (3 d orbital) to its NO-ligand (antibonding $\pi^\star$), the electron charge density of the molecule is altered and results in a rearrangement of the molecular structure: the NO rotates either by $90°$ with respect to the Fe-N-O bond yielding a so-called *side-on* configuration, known as metastable state SII in literature. Or, rotation by $180°$ results in an *isonitrosyl* state SI [24–27]. Accordingly, the reaction coordinate shown in Figure 2 is identified by the bonding angle of the NO ligand with respect to Fe-N-O [15] and two altered ground state potentials SI and SII must be added at $90°$ and $180°$.

Figure 3. Nitroprusside ion in its three structural isomers. GS: thermally stable ground state; SI, SII: light-induced metastable states. The arrows indicate the light-induced isomerization pathways and the corresponding wavelengths for SNP.
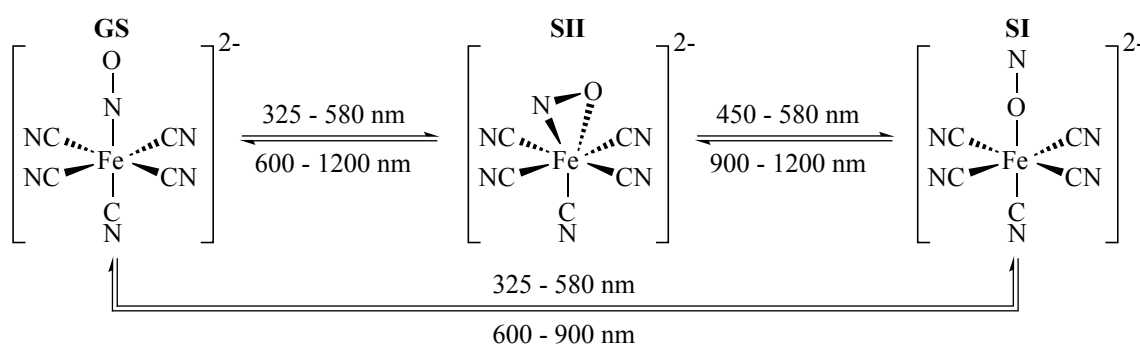

The photon energy for the isomerization process has been widely studied [6,24,26–29]. Isomerization is possible by exposure of SNP to light in the blue-green spectral range (350–580 nm). Remarkably, the system allows for complete optically induced backswitching in the red and near-infrared spectral range [30] as depicted by the specific wavelengths given in Figure 3 despite the possibility of a thermal relaxation from SI, SII to GS [2,7,24,31]. The activation energies for the thermal decay of SI and SII have been determined to $E_{A,I} = 0.68\,\text{eV}$ and $E_{A,II} = 0.52\,\text{eV}$ for SNP, respectively, resulting in lifetimes of $\tau_I = 154\,\mu s$ and $\tau_{II} = 0.18\,\mu s$ at room temperature and of $\tau > 10^{15}\,\text{s}$ at nitrogen temperatures [7,32,33]. The complex energy landscape that covers these structural findings have been confirmed by calculations using density functional theory (DFT) [28,34].

It has been shown that these specific features can be tuned widely by ligand substitution [4,5,35,36], while the basic photofunctionality is preserved [15]. For example, the lifetimes at room temperature can be prolongated from the microsecond regime in SNP to several seconds by substitution of ligands, e.g., in the $[Ru(NH_3)_4(H_2O)NO]Cl_3\cdot H_2O$ compound [37].

An equivalent molecular alteration is reported for the photofunctionality of the second important class of transition metal compounds, the polypyridine sulfoxide compounds. Here, a light-induced isomerization [38] is located at the SO group as depicted in Figure 4 for $[Ru(bpy)_2(OSO)]^+$ (OSO) [39,40]. The MLCT transition $\text{Ru}\,d\pi \rightarrow \text{bpy}\,\pi^\star$ is triggered by exposure to light of 380–440 nm [20,40]. In most sulfoxide compounds, a light-induced transfer from SI/SII to GS is not

observed, but can be enabled by using pySO as switching ligand [41]. In OSO, DFT calculations predict two metastable isomers, both having the SO rotated by $180°$. They only slightly differ in the bonding angles of the benzene ligand [40]. The prediction is in line with the observation of a two-fold exponential thermal relaxation behavior from SI/SII to GS yielding two distinctive activation energies [20] and showing no dependence of the relaxation time constants on the probing wavelength as it was studied for $\lambda = 352$ nm, 400 nm and 500 nm in Reference [42]. It is also supported by the similarities in the absorption spectra of SI and SII that cannot be distinguished with standard techniques [40]. Due to its high activation barrier of $E_{A,I} = 0.76$ eV and $E_{A,II} = 1.00$ eV for thermal relaxation, lifetimes of 1.6×10^3 s and 3.9×10^4 s, respectively, at room temperature are determined [20].

Figure 4. Scheme of the light-induced isomerization for $[Ru(bpy)_2OSO]^+$ from its ground state GS (left) to the metastable states SI/SII (right). For simplicity the metastable states are only depicted as one state in this scheme.
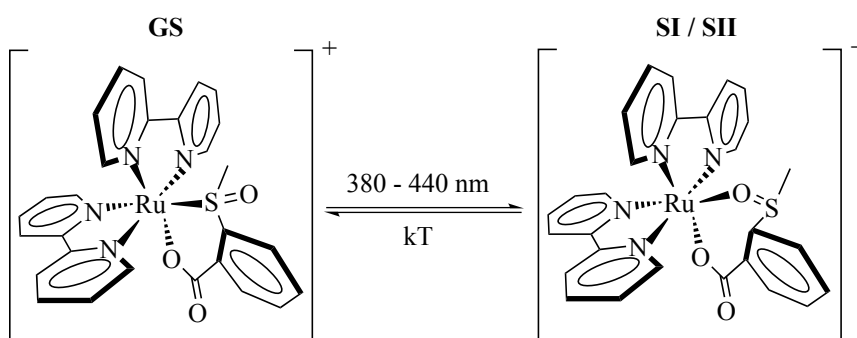

3. Two-Wave Mixing Phenomena in Transition Metal Compounds

Recording of holograms in media built from molecular transition metal compounds is rather different from the photophysical processes that underly absorption or index changes in classical holographic recording media. We first need to consider the bulk medium (in the order of several mm^3) to be composed of a homogeneous, three-dimensional distribution of single molecules characterized by concentration c. The latter is chosen such that intermolecular interactions as well as losses of the photon flux by absorption along the light propagation coordinate can be neglected. We further assume that the duration of light exposure τ is shorter than the isomerization time $\tau_{GS\to MS}$. This prevents us from the consideration of population phenomena (which will be discussed in the second part of this chapter).

The recording of an elementary hologram will be assumed as sketched in Figure 5a: The molecular sample is exposed to two coherent laser beams of wavelength λ designated by the wave vectors $\mathbf{k}_R$ and $\mathbf{k}_S$ yielding a spatially modulation distribution of intensity along the x-coordinate, $I(x) = (I_R + I_S)[1 - m\cos(Kx)]$, within the bulk. Here, m denotes the modulation depth $m = 2\sqrt{I_R \times I_S}/(I_R + I_S)$ with the respective intensities $I_{R,S}$ of reference and signal wave. The modulo of the wave vector $|\mathbf{K}| = 2\pi/\Lambda$ is the spatial frequency and Λ is the wavelength of the light pattern. Note, that $\mathbf{K} = \mathbf{k}_S - \mathbf{k}_R$ reflects the momentum conservation, *i.e.*, the Bragg condition.

Figure 5. (**a**) Scheme of hologram recording via two beams; (**b**) In SNP the illumination with a sinusoidal light pattern results in spatially modulated number densities ($c_{GS}(x)$, $c_{SI}(x)$, and $c_{SII}(x)$) leading to a modulation of the refractive index $n(x)$ and the absorption coefficient $\alpha(x)$.
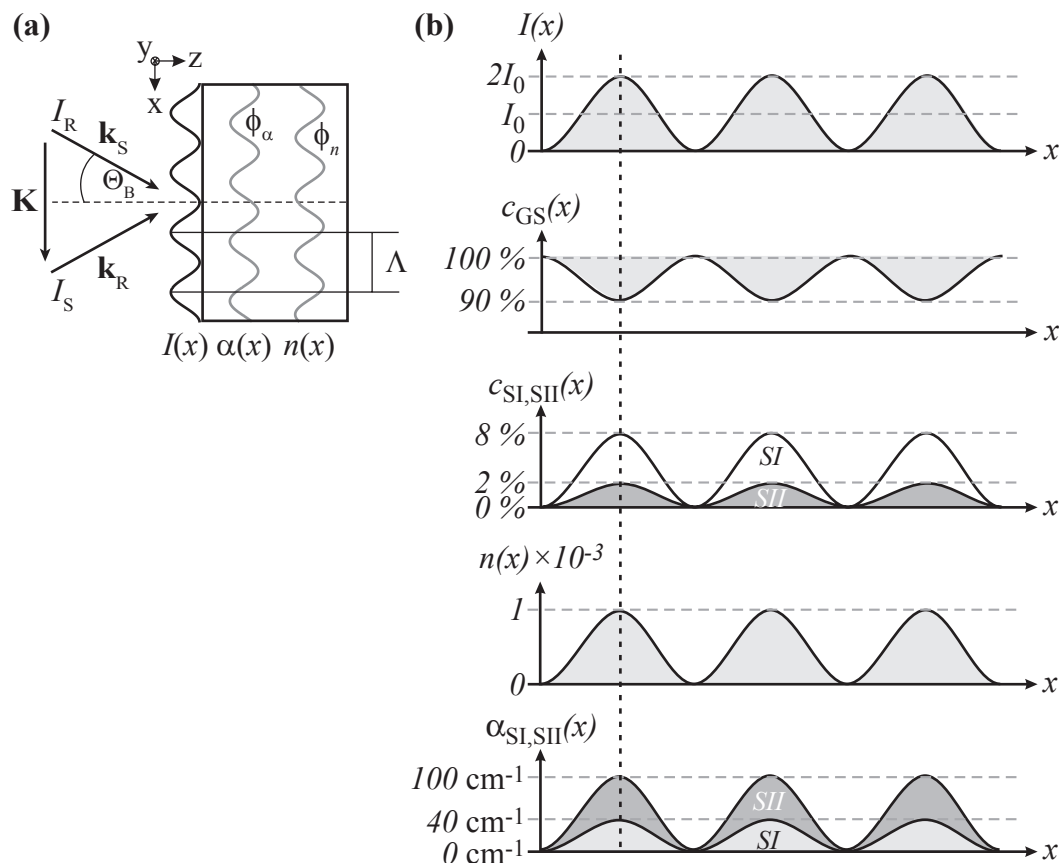
Let us now consider the response of the molecular compound on the incoming light pattern with SNP as an example (see Figure 5b). Light-induced linkage isomerization appears in the bright region of the light pattern $I(x)$, *i.e.*, spatially modulated number densities $c_{GS}(x)$ phase-shifted by π with respect to $I(x)$, and $c_{SI,SII}(x)$ in-phase with $I(x)$, respectively, appear. The alteration of the electronic and molecular structure is accompanied with changes in the molecular susceptibility. Via Lorentz–Lorenz relation, changes in the absorption features and refractive index of molecular compounds can be expected. Therefore, we can assume that the spatially modulated isomerization is linked to a spatially modulated refractive index $n_{SI,SII}(x)$ and absorption coefficient $\alpha_{SI,SII}(x)$ that are in-phase with the light pattern and feature the same spatial frequency. It means that non-phase-shifted, mixed absorption and phase gratings are recorded. Appropriate thicknesses of the molecular compound allow for volume holography.

This recording scheme was experimentally investigated in detail for spatial modulation of metastable state SI [3]. Holographic gratings were recorded using SNP single crystals with typical dimensions of $10 \times 10\,\text{mm}^2$ and thicknesses between 100 and 500 μm (*cf.* Figure 1). The studies were performed in a liquid-nitrogen filled Dewar at temperatures of $T \approx 100\,\text{K}$, thus enabling a lifetime of the switched states of $\tau_{SI} > 10^9\,\text{s}$ [6]. The increase of the lifetime is inevitably necessary to reach large changes of the molecular concentrations in the isomerized states via population phenomena resulting in large amplitudes

δn, $\delta\alpha$. As a result, the presence of a mixed grating with dominating contribution of the amplitude of refractive-index change (up to $\delta n \propto 10^{-2}$) and a phase-shift between absorption/index grating and the light pattern of $\Phi_{n,\alpha} \approx 0$ could be revealed via four-wave mixing techniques [3]. Furthermore, related nonlinear photorefractive phenomena including photo-induced polarization-isotropic and polarization-anisotropic light scattering [43,44], the recording of gratings with mutually orthogonal polarized waves [45] and the interaction of photorefraction and spectroscopy [46] were demonstrated. Besides recording of gratings via isomerization, we note that the inverse process is also possible, *i.e.*, spatial homogeneous isomerization of the molecular crystal followed by hologram recording via the optical transfer of the isomer into its ground state [1]. Furthermore, population saturation phenomena yielding a temporal alteration of the sinusoidal grating could be verified [47].

4. Holographic Media Composed of Transition Metal Compounds: Specifications

According to the photofunctionality of transition metal compounds (Section 2) and the unique hologram recording mechanism (Section 3), we will now focus on the specifications that can be expected for holographic materials that are composed of transition metal compounds. These specifications are to be discussed inevitably, because they finally determine the properties of any of the mentioned applications (Section 1). Considering the nitroprusside and sulfoxide class, we will particularly deal with the following measures: hologram modulation depth, hologram sensitivity, spectral hologram sensitivity, hologram lifetime and large scale thick media.

4.1. Hologram Modulation Depth

The hologram modulation depth n_1, α_1 is a key measure for hologram recording, because it quadratically determines the diffraction efficiency η in mixed phase and amplitude volume gratings [48]. It is related to the mean value of the refractive index n_0 and absorption coefficient α_0 via $n(x) = n_0 + n_1 \cos(Kx)$ and $\alpha(x) = \alpha_0 + \alpha_1 \cos(Kx)$. Here, the local photorefractive and photochromic responses ($\Phi_n, \Phi_\alpha = 0$) valid for transition metal compounds (see Section 3) are taken into account and higher orders of the Fourier expansion are neglected. By considering the hologram recording mechanism (Section 3), the maximum amplitudes of the changes of refractive index δn and absorption coefficient $\delta\alpha$ are related to the modulation depth by a factor of two: $2n_1 = \delta n$, $2\alpha_1 = \delta\alpha$.

In SNP, both, photochromism and photorefractivity are very pronounced, e.g. the maximum of the light-induced absorption change is in the order of $\delta\alpha \approx 400$ cm^{-1} [6,28] and of the refractive-index change $\delta n \approx 10^{-2}$ measured for single crystalline SNP, respectively [2,3,43,46]. Figure 6a illustrates the development of the absorption spectrum for an unexposed (solid line, GS) and an exposed (dashed, SI + SII) SNP crystal with $\lambda = 457.9$ nm light as a function of probing wavelength [49]. Here, the light polarization was chosen to be parallel to the crystallographic c-axis in order to suppress the dominating influence of photoinduced light-scattering [43].

The absorption increases in the near-infrared and decreases in the blue-green spectral range. In the view of a pure amplitude grating, a maximum hologram modulation depth m can be obtained for $\lambda \approx 750$ nm and $\lambda \approx 450$ nm. In order to minimize the contribution of absorption gratings, recording of phase holograms should be performed near to the isosbestic point at about 550 nm. Figure 6b shows

the results of the index modulation amplitude δn for recording using two beams of $\lambda = 514.5\,\text{nm}$ as a function of the modulation depth of the light fringe pattern. A maximum is observed, if $m \approx 0.8$, *i.e.*, for the case that the intensities of reference and signal waves slightly differ. These index amplitudes allow for diffraction efficiencies of more than 90% in crystals as thin as 200 μm [3].

Figure 6. (**a**) Absorption spectra of a b-cut SNP single crystal for light polarization parallel to its c-axis. The solid line represents absorbance of GS and the dashed line of SI + SII subsequent to optical excitation with $\lambda = 457.9\,\text{nm}$ light; (**b**) Amplitude of index modulation as a function of the modulation depth of the fringe pattern ($\lambda = 514.5\,\text{nm}$).
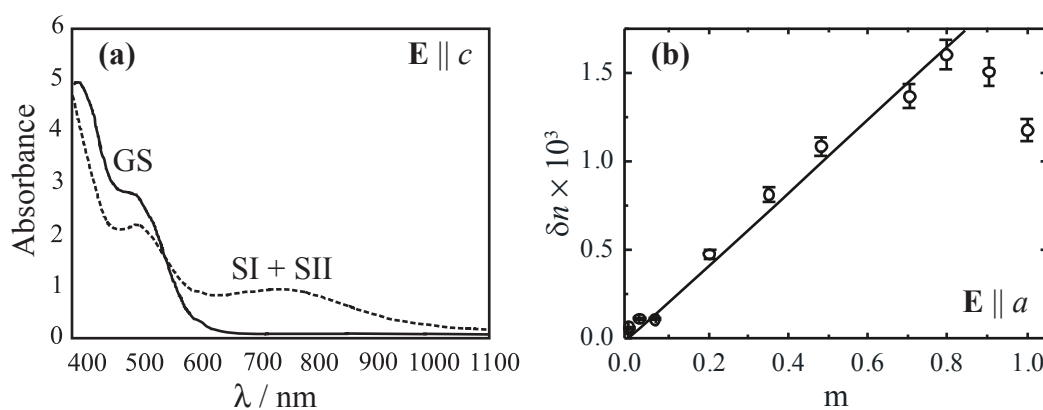

Besides nitroprussides, polypyridine sulfoxide compounds are dealt with as promising photochromic transition metal compound. Different compounds were already studied [5,14,16,50–52] and demonstrate a very pronounced photochromism. Changes of the extinction coefficient up to $\delta\epsilon(\lambda = 504\,\text{nm}) = \delta\alpha/c = (1.6 \pm 0.1) \times 10^4\,\text{M}^{-1}\,\text{cm}^{-1}$ were reported for [Ru(bpy)$_2$(OSO)]·PF$_6$ dissolved in propylene carbonate (PC) with c being the concentration of the solution [20].

Figure 7a depicts the VIS absorption spectra of such a solution with $c = 0.20\,\text{mM}$. During exposure to 405 nm light, two new absorption maxima build up at 352 nm and 500 nm, which are assigned to SI + SII [40] with respect to the ground state (solid line), while the absorption at 400 nm vanishes. After reaching saturation (dashed line) the absorption at 400 nm is only given by the overlap of absorption bands assigned to SI + SII [20]. The process is reversed by thermal activated relaxation from SI + SII to GS as indicated by the dotted line representing a spectrum after 20 minutes of relaxation at room temperature. The inset shows pictures of a solution with 0.88 mM OSO in its GS (left) and SI + SII (right). The concentration of the solution was increased for optimization of the contrast in the pictures ($\alpha = \epsilon \times c$). Selected kinetics of the relaxation process at room temperature are presented in Figure 7b. No spectral dependence of the relaxation time constant in the VIS spectral range can be found, underlining the proposed structural similarities between SI and SII discussed in Section 2.

The related change of the refractive index can be at least estimated by applying Kramers–Kronig relation [42]. In Figure 8 the experimental change of the absorption coefficient (dashed line) and the calculated refractive-index change (solid) for a 0.88 mM PC solution of OSO are presented. In the visible spectral range $\delta n \approx 10^{-5}$ with a maximum of 3.9×10^{-5} at 468 nm can be expected. It is worth noting that δn like $\delta\alpha$ are proportional to the concentration of the solution.

Figure 7. Absorption of 0.20 mM OSO dissolved in PC. (**a**) Absorption spectra for GS (solid line), subsequent to exposure to 405 nm light (SI + SII, dashed), after 20 minutes relaxation at room temperature after exposure (dotted). Inset: Pictures of a 0.88 mM solution; (**b**) Thermal relaxation kinetics of the three dominant VIS absorption bands, $t = 0$ s equals the spectrum SI + SII in the left frame, $t \to \infty$ equals GS.
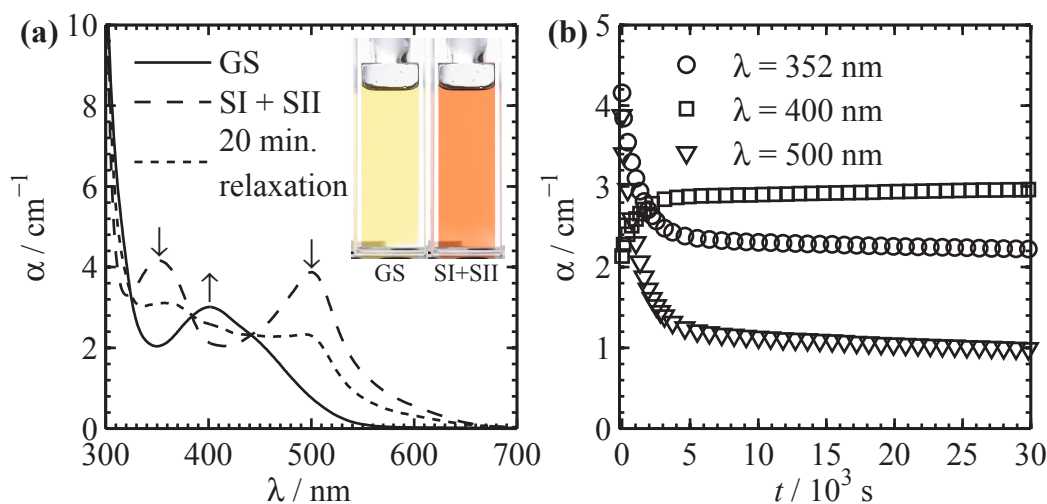
4.2. Hologram Sensitivity

The hologram sensitivity S is defined by the amplitude of the material response ($\delta\alpha$, δn) normalized on the light exposure $Q = I \times \tau$, the product of recording intensity I and characteristic time constant τ for the build up of the response. This measure was introduced by Günter in 1982 for photorefractive crystals $S = \delta n/(I \times \tau)$ [53] and is a measure for the velocity of recording efficient holograms. It can easily be adapted to molecular compounds $S_n = \delta n/(I \times \tau \times c)$, with the concentration c and to a molecular photochromic sensitivity $S_\alpha = \delta\alpha/(I \times \tau \times c)$.

We have summarized the values for the photochromic and photorefractive sensitivities for nitroprusside single crystals and solutions as well as for sulfoxide solutions in Table 2. The respective values are given for the wavelength representing the maximum hologram modulation depth. (Except for OSO, where the values were determined at exactly that wavelength, all values are given for laser wavelengths nearby to the maximum change or typical wavelength used in experiments.) For comparison, values for the photorefractive crystal lithium niobate are given, as well. It demonstrates that both transition metal compounds feature larger or at least comparable values of the sensitivity. Also we like to note, that an increase in five orders of magnitude is found by comparing OSO to SNP. Thereby, the further media development of sulfoxide compounds for holography remains very promising.

In addition to the tremendous sensitivities, the transition metal compounds presented in this work feature a fast response time of the isomerization to light exposure: The isomerization has been verified to take place within less than 300 fs for SNP [9] and 150 ps for OSO [19]. This offers the opportunity for application in ultrafast devices using femto- or picosecond pulses.

Figure 8. Experimental absorption change (dashed line) and estimated refractive index change (solid) for a 0.88 mM OSO PC solution in the visible spectral range.
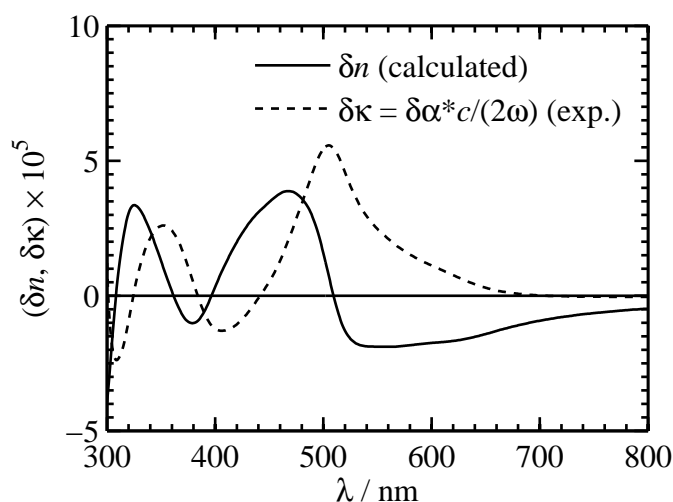

Table 2. Photochromic S_α and photorefractive sensitivities S_n for SNP and OSO at wavelength λ_α, λ_n. Values marked with a star ($\star$) are estimated via Kramers–Kronig relation. For comparison sensitivities for photorefractive lithium niobate are given.

Compound	λ_α (nm)	S_α (cm J^{-1} M^{-1})	λ_n (nm)	S_n (cm^2 J^{-1} M^{-1})	Reference
[Ru(bpy)$_2$OSO]$^+$ ($T = 318$ K)	504.0	10.5×10^4	468.0	$3.0 \times 10^{-1,\star}$	[20]
Na$_2$[Fe(CN)$_5$NO]·2H$_2$O ($T = 80$ K)			514.5	1.7×10^{-6}	[3,49]
(dissolved in H$_2$O, $T = 300$ K)	632.8	4.7×10^{-1}			[33]
LiNbO$_3$			514.5	2.9×10^{-7}	[54]
(various dopands)			632.8	1.2×10^{-13}	[55]

4.3. Hologram Lifetime

The hologram lifetime is determined by the self-decay of the index/absorption modulation down to the $1/e$-value of the maximum diffraction efficiency after finishing the recording process. It may be accelerated by exposure of the hologram to a spatial homogeneous light distribution for purposes of hologram reconstruction. Depending on the desired storage application, there are different demands on the lifetime of recorded information spanning from a few nanoseconds for e.g., display technologies up to more than 500 years for storage applications. It should be noted that the hologram lifetime is temperature dependent, *i.e.*, decreasing with increasing temperature.

Figure 9 exemplarily shows three compounds and their lifetimes at a temperature of 300 K: More than eleven orders of magnitude in lifetime can be covered by the choice of the molecular compound. On the long living side, sulfoxide compounds feature lifetimes in the range of several hours for the metastable isomers [20,56], whereas the nitroprusside compounds cover the range from 1.1×10^{-7} s to several seconds at room temperature [33,37,57,58].

Figure 9. Lifetimes of the two metastable isomers for three exemplary compounds: A span from 1.1×10^{-7} s [33] to 3.5×10^4 s [20] can be covered by the choice of the sulfoxide or nitroprusside compound.
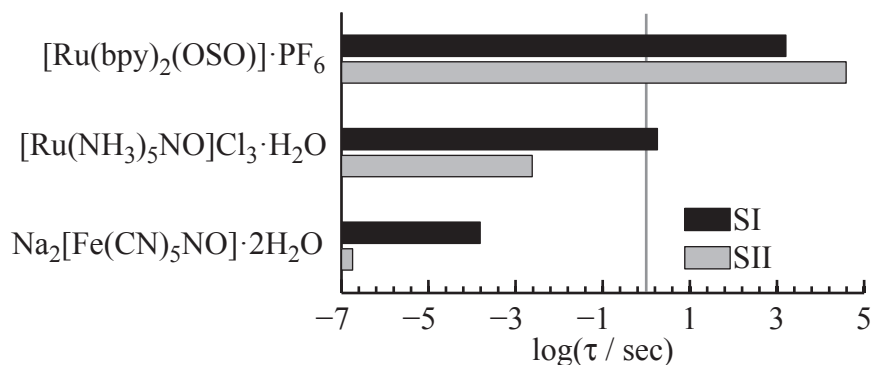
4.4. Spectral Hologram Sensitivity

The spectral hologram sensitivity relates the hologram sensitivity to the recording/read-out wavelength. It is an important measure for applications that require hologram recording features at a particular wavelength. Examples are dynamical wavelength filters for telecommunication devices operating in the $1.55\,\mu$m spectral range or holographic displays with desired hologram responses in the blue, green and red spectral range.

According to the properties of transition metal compounds, the spectral range of hologram sensitivity commonly is already quite large and covers 50–100 nm (see Section 4.1). In addition, we like to report here on the possibility of tailoring the spectral hologram sensitivity either by substitution of specific ligands or by replacement of the dielectric environment. This yields a shift of the maximum of the hologram sensitivity by several hundred nanometers.

Nitroprussides are very small molecules (13 atoms for sodium nitroprusside (SNP), see Figure 3), and thus, the substitution of one single atom has major consequences to all features like absorption spectra, sensitivity, lifetime, etc. The spectral sensitivity for the isomerization pathways for SNP are reported to be shifted by more than 200 nm to the red ($\lambda_{GS} = 714$ nm) in $[Pt(NH_3)_4Cl(NO)]\cdot Cl_2$ [59]. Table 3 summarizes the central wavelengths of the lowest lying MLCT absorption in GS and SI + SII for selected transition metal compounds illustrating the tuning range from UV to NIR for the GS absorption. Sulfoxide compounds are slightly larger (about 60 atoms, see Figure 4) and, therefore, a selective alteration of specific features can be achieved by the substitution of a single atom or a ligand. Rack *et al.* have demonstrated systematic studies on the substitution of the non-photofunctional ligand L2 in $[Ru(tpy)(L2)(DMSO)]^{2+}$ (tpy is 2,2':6',2''-terpyridine and DMSO is dimethylsulfoxide) compounds. Here, the spectral sensitivity can be tuned by usage of L2 = Me-pic (6-methyl-2-pyridinecarboxylate) instead of bpy (2,2'-bipyridine) from 419 nm to 447 nm for the lowest energy MLCT in GS [16,60]. Even a complete turning-off of the photofunctionality by usage of malonate or acetylacetonate as L2 ligand was reported [16]. Shifting the absorption maximum further into the red has been performed by substitution of one non-photofunctional ligand bpy (2,2'-bipyridine) in $[Ru(bpy)_2(OSO)]^+$ with biq (2,2'-biquinoline). This substitution shifts the absorption from 396 nm [40] by nearly 80 nm to 474 nm [61].

Table 3. Central wavelength of the lowest lying MLCT absorption band in the ground (GS) and metastable states (SI + SII) for selected transition metal compounds

Compound	$\lambda_{\mathrm{max,GS}}$ (nm)	$\lambda_{\mathrm{max,SI + SII}}$ (nm)	Reference
$Na_2[Fe(CN)_5NO]\cdot H_2O$	495	755	[8]
$[Pt(NH_3)_4Cl(NO)]\cdot Cl_2$	714	1020	[59]
$[Ru(bpy)_2(OSO)]^+$	401	499	[20]
$[Ru(bpy)_2(R-OSO)]^+$	401	500	[56]
$[Ru(bpy)(biq)(OSO)]^+$	474	572	[61]
$[Ru(bpy)_2(pySO)]^+$	370	472	[41]
$[Ru(tpy)(bpy)(DMSO)]^{2+}$	419	480	[62]
$[Ru(tpy)(Me-pic)(DMSO)]^+$	447	506	[60]
$[Ru(tpy)(acac)(DMSO)]^{2+}$	468	–	[16]

At this point we like to address the question whether other features, besides the spectral hologram sensitivity, are affected. Regarding L2, it has been shown that the ligand has only a minor influence on the lifetime of the metastable states. Vice versa, we have demonstrated that the exchange of R in $[Ru(bpy)_2(R-OSO)]^+$ influences the lifetime, but not the sensitivity or the absorption spectra of the compound [20,56]. These adaptabilities and their consequences can be understood by the structure of the compounds and the MLCT transition itself: After the light absorption, an electron is excited to an orbital localized at a non-photofunctional ligand, e.g., bpy, tpy or acac, and, hence, the required photon energy for the MLCT is directly modified by exchange of that ligand. The exchange of R being bonded to the photofunctional SO ligand directly influences the bonding strength of the latter to the metal in the ground and metastable states.

Finally, we address the possibility of tailoring the spectral hologram sensitivity by adjustment of the dielectric environment, e.g., $[Ru(bpy)_2(OSO)]^+$ dissolved in different solvents (propylene carbonate, methanol or dichloromethane). Although it is in principle possible, it is not of interest for the field of hologram media development: the spectral position of the maximum absorption band can only be influenced in range of about 3%.

4.5. Building Up Large Scale Thick Media

This final subsection covers the last important step towards a successful hologram media development using transition metal compounds. Large scale media with areal dimensions $\gg 1\,cm^2$ are of importance for any type of holographic imaging applications, e.g., holographic display technologies. Thick media featuring thicknesses $\gg 1\,mm$ particularly imply the possibility to record volume holograms, *i.e.*, large values of the diffraction efficiency can be reached. In addition, all devices have in common the need for cheap and easy production and the possibility for large scales and small dimensions—an industrial requirement.

These media demands can be met by transition metal compounds due to the possibility for embedding the molecules within different dielectric environments. As mentioned, the photofunctionality of these compounds is based on an unimolecular photochemical reaction and, therefore, does not require an ordered environment or long-range charge-transport mechanism as it is the case for crystals featuring the photorefractive effect.

Over the past decade, the class of NP was mostly studied in single crystals revealing a high performance in all key features. For overcoming the costly crystal growing process, SNP has been proven to preserve its photofunctionality in aqueous solutions [33]. Here, a pronounced photochromic response to ns-laser pulses with relaxation constants comparable to single crystals was observed. Also powder samples and NP embedded in xerogels were successfully studied [17]. However, electrostatic attachment of monolayers of SNP to TiO_2 films (see Figure 10) reveals a modified photofunctionality and no isomerization could be observed at room temperature and at 80 K by means of FT-IR spectroscopy. Instead a release of NO was ascribed to a two-step process most likely involving the isomerization as intermediate step [18].

Figure 10. SNP electrostatically attached to a thin TiO_2 film on a Si substrate material.
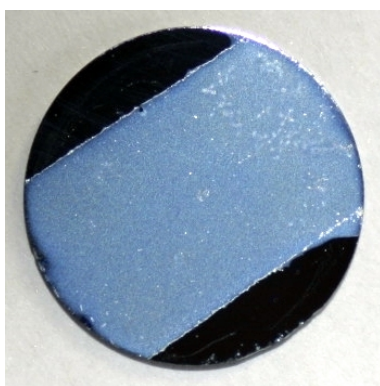

The sulfoxide compounds has been intensively studied in microcrystalline powders and a wide range of solvents [16,61] for the influence of the solvent on the photofunctionality of the compounds. Up to now there are no reports on monolayers of SO on a thin film, but the environment used in Reference [18] could be modified to hold the positively charged OSO instead of negatively charged NP [63]. Unlike SNP, that compound should not alter its photofunctionality, while being attached to the TiO_2, due to its larger size and, therefore, due to less influence of the electrostatic spacer it is attached to.

Only recently, we succeeded in embedding OSO into a polymer (PDMS) yielding a flexible and mechanically stable material of good optical quality. Pictures of the sample are depicted in Figure 11. The right half of the sample was irradiated by white light of a halogen lamp for demonstration of the photofunctionality. The color of the sample changes from yellow (GS) to brownish/red (SI + SII) like it is known for the fluid samples (*cf.* Figure 7). It was shown that besides small shifts of the absorption bands and a reduction of the extinction coefficient by less than one order of magnitude, the photofunctionality is completely preserved. The thermal stability of SI + SII is increased by more than one order of magnitude compared to solutions. PDMS seems to be a promising environment because of its easy and cheap production process and the possibility for tuning the magnitude of the optical features by the

concentration of the compound. As shown in the side view in Figure 11, the polymer environment offers a unique mechanical stability and flexibility.

Figure 11. OSO embedded in PDMS. The right half of the sample was irradiated by white light of a halogen lamp for demonstration of the photofunctionality.
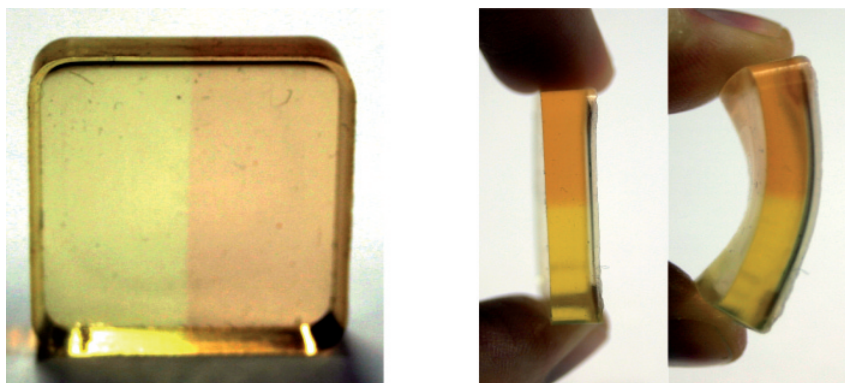
5. Conclusions

The nanoscopic bottom-up approach from functional transition metal compounds to advanced materials for holography turned out to be highly attractive and successful for the development of novel holographic media. It is very promising for a variety of visionary holographic applications that require either a huge photosensitivity, a high spatial resolution and low-cost materials at large media dimensions. Also the research field dealing with the nonlinear optical properties of transition metal compounds strongly developed in recent years by solving a multitude of open physical and physico-chemical questions, such as the relation between structural modification of small molecules and the macroscopic susceptibility beyond Kramers–Kronig relation. Some of them still require research. Particularly from the view point of material sciences, active research addresses the embedding of transition metal compounds into large-scale dielectric matrices by keeping the photofunctionality as well as a high optical quality (*laser grade*) of the medium. Also, the combination of the photofunctionality with the reported electrochromic response of sulfoxides seems to be promising for further development: optical recording in the sub-nano- to picosecond time domain can be combined with an electrical erasure in the millisecond regime [64].

In a more general view, the novel media can already be classified with regard to common holographic recording materials. We here follow the scheme presented in Reference [65]. Media built from transition metal compounds of the nitroprusside class allow for the recording of dynamic, thick, phase holograms either in transmission or reflection geometry. They represent reversible media without the necessity for chemical (post-)processing. Media of sulfoxides are to be preferred for the recording of dynamic, thick, amplitude transmission or reflection gratings. Thereby, they are of importance for the field of holographic interferometry [66–69]. Despite so, all transition metal compound media have tremendous impact for the developing field of ultrafast holography because of their unique structural response time in the order of sub-picoseconds.

Acknowledgements

References

1. Haussühl, S.; Schetter, G.; Woike, T. Nitroprussides, a new group of materials for holographic information-storage on the basis of metastable electronic states. *Opt. Commun.* **1995**, *114*, 219–222.

2. Woike, T.; Haussühl, S.; Sugg, B.; Rupp, R.A.; Beckers, J.; Imlau, M.; Schieder, R. Phase gratings in the visible and near-infrared spectral range realized by metastable electronic states in $Na_2[Fe(CN)_5NO]\cdot2\,H_2O$. *Appl. Phys. B* **1996**, *63*, 243–248.

3. Imlau, M.; Haussühl, S.; Woike, T.; Schieder, R.; Angelov, V.; Rupp, R.A.; Schwarz, K. Holographic recording by excitation of metastable electronic states in $Na_2[Fe(CN)_5NO]\cdot2H_2O$: a new photorefractive effect. *Appl. Phys. B* **1999**, *68*, 877–885.

4. Gütlich, P.; Garcia, Y.; Woike, T. Photoswitchable coordination compounds. *Coord. Chem. Rev.* **2001**, *219*, 839–879.

5. Coppens, P.; Novozhilova, I.; Kovalevsky, A. Photoinduced linkage isomers of transition-metal nitrosyl compounds and related complexes. *Chem. Rev.* **2002**, *102*, 861–883.

6. Woike, T.; Kirchner, W.; Schetter, G.; Barthel, T.; Hyungsang, K.; Haussühl, S. New information-storage elements on the basis of metastable electronic states. *Opt. Commun.* **1994**, *106*, 6–10.

7. Zöllner, H.; Woike, T.; Krasser, W.; Haussühl, S. Thermal decay of laser-induced long living metastable electronic states in $Na_2[Fe(CN)_5NO]\cdot2H_2O$ single-crystals. *Z. Kristallogr.* **1989**, *188*, 139–153.

8. Schaniel, D.; Schefer, J.; Imlau, M.; Woike, T. Light-induced structural changes by excitation of metastable states in $Na_2[Fe(CN)_5NO]\cdot2H_2O$ single crystals. *Phys. Rev. B* **2003**, *68*, 104108:1–10418:11.

9. Schaniel, D.; Nicoul, M.; Woike, T. Ultrafast reversible ligand isomerisation in $Na_2[Fe(CN)_5NO]\cdot2H_2O$ single crystals. *Phys. Chem. Chem. Phys.* **2010**, *12*, 9029–9033.

10. Cotter, D.; Manning, R.J.; Blow, K.J.; Ellis, A.D.; Kelly, A.E.; Nesset, D.; Phillips, I.D.; Poustie, A.J.; Rogers, D.C. Nonlinear optics for high-speed digital information processing. *Science* **1999**, *286*, 1523–1528.

11. O'Mahony, M.J.; Politi, C.; Klonidis, D.; Nejabati, R.; Simeonidou, D. Future optical networks. *J. Lightwave Technol.* **2006**, *24*, 4684–4696.

12. Haque, S.A.; Nelson, J. Toward organic all-optical switching. *Science* **2010**, *327*, 1466–1467.

13. Straight, S.D.; Liddell, P.A.; Terazono, Y.; Moore, T.A.; Moore, A.L.; Gust, D. All-photonic molecular XOR and NOR logic gates based on photochemical control of fluorescence in a fulgimide-porphyrin-dithienylethene triad. *Adv. Funct. Mater.* **2007**, *17*, 777–785.

14. Vos, J.G.; Pryce, M.T. Photoinduced rearrangements in transition metal compounds. *Coord. Chem. Rev.* **2010**, *254*, 2519–2532.

15. Schaniel, D.; Imlau, M.; Weisemoeller, T.; Woike, T.; Kramer, K.W.; Güdel, H.U. Photoinduced nitrosyl linkage isomers uncover a variety of unconventional photorefractive media. *Adv. Mater.* **2007**, *19*, 723–726.

16. Rack, J.J. Electron transfer triggered sulfoxide isomerization in ruthenium and osmium complexes. *Coord. Chem. Rev.* **2009**, *253*, 78–85.

17. Schuy, A.; Woike, T.; Schaniel, D. Photoisomerisation in single molecules of nitroprusside embedded in mesopores of xerogels. *J. Sol-Gel Sci. Technol.* **2009**, *50*, 403–408.

18. Dieckmann, V.; Imlau, M.; Taffa, D.H.; Walder, L.; Lepski, R.; Schaniel, D.; Woike, T. Phototriggered NO and CN release from $[Fe(CN)_5NO]^{2-}$ molecules electrostatically attached to TiO_2 surfaces. *Phys. Chem. Chem. Phys.* **2010**, *12*, 3283–3288.

19. McClure, B.A.; Rack, J.J. Ultrafast spectroscopy of a photochromic ruthenium sulfoxide complex. *Inorg. Chem.* **2011**, *50*, 7586–7590.

20. Dieckmann, V.; Eicke, S.; Rack, J.J.; Woike, T.; Imlau, M. Pronounced photosensitity of molecular $[Ru(bpy)_2(OSO)]^+$ solutions based on two photoinduced linkage isomers. *Opt. Express* **2009**, *17*, 15052–15060.

21. Balzani, V.; Bergamini, G.; Campagna, S.; Puntoriero, F. Photochemistry and photophysics of coordination compounds: Overview and general concepts. *Top. Curr. Chem.* **2007**, *280*, 1–36.

22. Demas, J.N. Photophysical pathways in metal-complexes. *J. Chem. Educ.* **1983**, *60*, 803–808.

23. Watts, R.J. Ruthenium polypyridyls—A case-study. *J. Chem. Educ.* **1983**, *60*, 834–842.

24. Woike, T.; Krasser, W.; Zöllner, H.; Kirchner, W.; Haussühl, S. Population-dynamics of the two light-induced metastable states in $Na_2[Fe(CN)_5NO]\cdot 2H_2O$ single crystals. *Z. Phys. D* **1993**, *25*, 351–356.

25. Schaniel, D.; Woike, T. Necessary conditions for the photogeneration of nitrosyl linkage isomers. *Phys. Chem. Chem. Phys.* **2009**, *11*, 4391–4395.

26. Pressprich, M.R.; White, M.A.; Vekhter, Y.; Coppens, P. Analysis of A metastable electronic excited-state of sodium-nitroprusside by X-ray crystallography. *J. Am. Chem. Soc.* **1994**, *116*, 5233–5238.

27. Carducci, M.D.; Pressprich, M.R.; Coppens, P. Diffraction studies of photoexcited crystals: Metastable nitrosyl-linkage isomers of sodium nitroprusside. *J. Am. Chem. Soc.* **1997**, *119*, 2669–2678.

28. Schaniel, D.; Schefer, J.; Delley, B.; Imlau, M.; Woike, T. Light-induced absorption changes by excitation of metastable states in $Na_2[Fe(CN)_5NO]\cdot 2H_2O$ single crystals. *Phys. Rev. B* **2002**, *66*, 085103:1–085103:10.

29. Woike, T.; Krasser, W.; Bechthold, P.S.; Haussuhl, S. Extremely long-living metastable state of Na$_2$[Fe(CN)$_5$NO]·2H$_2$O single-crystals—optical-properties. *Phys. Rev. Lett.* **1984**, *53*, 1767–1770.

30. Rüdlinger, M.; Schefer, J.; Chevrier, G.; Furer, N.; Güdel, H.U.; Haussühl, S.; Heger, G.; Schweiss, P.; Vogt, T.; Woike, T.; Zöllner, H. Light-induced structural-changes in sodiumnitroprusside (Na$_2$(Fe(CN)$_5$NO)·2D$_2$O) at 80 K. *Z. Phys. B* **1991**, *83*, 125–130.

31. Woike, T.; Imlau, M.; Haussühl, S.; Rupp, R.A.; Schieder, R. Photorefractive behavior of Ba[Fe(CN)$_5$NO]·3H$_2$O in the red and near-infrared spectral range. *Phys. Rev. B* **1998**, *58*, 8411–8415.

32. Schaniel, D.; Woike, T.; Tsankov, L.; Imlau, M. Evidence of four light-induced metastable states in iron-nitrosyl complexes. *Thermochim. Acta* **2004**, *429*, 19–23.

33. Schaniel, D.; Woike, T.; Merschjann, C.; Imlau, M. Transient kinetics of light-induced metastable states in single crystals and aqueous solutions of Na$_2$[Fe(CN)$_5$NO]·2H$_2$O. *Phys. Rev. B* **2005**, *72*, 195119:1–195119:5.

34. Delley, B.; Schefer, J.; Woike, T. Giant lifetimes of optically excited states and the elusive structure of sodiumnitroprusside. *J. Chem. Phys.* **1997**, *107*, 10067–10074.

35. Zöllner, H.; Krasser, W.; Woike, T.; Haussühl, S. The existence of light-induced long-lived metastable states in different X$_n$[Fe(CN)$_5$NO]·yH$_2$O crystals, powders and solutions. *Chem. Phys. Lett.* **1989**, *161*, 497–501.

36. Ookubo, K.; Morioka, Y.; Tomizawa, H.; Miki, E. Vibrational spectroscopic study of light-induced metastable states of ethylenediaminenitrosylruthenium(II) complexes. *J. Mol. Struct.* **1996**, *379*, 241–247.

37. Schaniel, D.; Woike, T.; Delley, B.; Boskovic, C.; Biner, D.; Kramer, K.W.; Güdel, H.U. Long-lived light-induced metastable states in *trans*-[Ru(NH$_3$)$_4$(H$_2$O)NO]Cl$_3$·H$_2$O and related compounds. *Phys. Chem. Chem. Phys.* **2005**, *7*, 1164–1170.

38. Smith, M.K.; Gibson, J.; Young, C.; Broomhead, J.; Junk, P.; Keene, F. Photoinduced ligand isomerization in dimethyl sulfoxide complexes of ruthenium(II). *Eur. J. Inorg. Chem.* **2000**, *2000*, 1365–1370.

39. Butcher, D.P.; Rachford, A.A.; Petersen, J.L.; Rack, J.J. Phototriggered S → O isomerization of a ruthenium-bound chelating sulfoxide. *Inorg. Chem.* **2006**, *45*, 9178–9180.

40. McClure, B.A.; Mockus, N.V.; Butcher, D.P.; Lutterman, D.A.; Turro, C.; Petersen, J.L.; Rack, J.J. Photochromic ruthenium sulfoxide complexes: Evidence for isomerization through a conical intersection. *Inorg. Chem.* **2009**, *48*, 8084–8091.

41. McClure, B.A.; Rack, J.J. Two-color reversible switching in a photochromic ruthenium sulfoxide complex. *Angew. Chem., Int. Ed.* **2009**, *48*, 8556–8558.

42. Dieckmann, V. Lichtinduzierte Isomerisierung in Sulfoxid- und Nitrosyl-Komplexen: Phtoosensitivität und Modifikation (In German). Ph.D. Dissertation, Universität Osnabrück, Osnabrück, Germany, 2010.

43. Imlau, M.; Woike, T.; Schieder, R.; Rupp, R.A. Holographic scattering in centrosymmetric Na$_2$[Fe(CN)$_5$NO]·2H$_2$O. *Phys. Rev. Lett.* **1999**, *82*, 2860–2863.

44. Imlau, M.; Schieder, R.; Rupp, R.A.; Woike, T. Anisotropic holographic scattering in centrosymmetric sodium nitroprusside. *Appl. Phys. Lett.* **1999**, *75*, 16–18.

45. Imlau, M.; Woike, T.; Schieder, R.; Rupp, R.A. Holographic recording with orthogonally polarized waves in centrosymmetric $Na_2[Fe(CN)_5NO] \cdot 2H_2O$. *Europhys. Lett.* **2001**, *53*, 471–477.

46. Imlau, M.; Woike, T.; Schaniel, D.; Schefer, J.; Fally, M.; Rupp, R.A. Light-induced extinction originating from holographic scattering. *Opt. Lett.* **2002**, *27*, 2185–2187.

47. Fally, M.; Imlau, M.; Rupp, R.A.; Ellabban, M.A.; Woike, T. Specific recording kinetics as a general property of unconventional photorefractive media. *Phys. Rev. Lett.* **2004**, *93*, 243903:1–243903:4.

48. Kogelnik, H. Coupled wave theory for thick hologram gratings. *Bell Syst. Tech. J.* **1969**, *48*, 2909–2947.

49. Imlau, M. Der photorefraktive Effekt, holographische Informationsspeicherung und die Entdeckung holographischer Streuung in zentrosymmetrischen Kristallen (In German). Ph.D. Dissertation, Universität zu Köln, Cologne, Germany, 2000.

50. Nakai, H.; Isobe, K. Photochromism of organometallic compounds with structural rearrangement. *Coord. Chem. Rev.* **2010**, *254*, 2652–2662.

51. Juris, A.; Balzani, V.; Barigelletti, F.; Campagna, S.; Belser, P.; von Zelewsky, A. Ru(II) polypyridine complexes: Photophysics, photochemistry, eletrochemistry, and chemiluminescence. *Coord. Chem. Rev.* **1988**, *84*, 85–277.

52. Calligaris, M. Structure and bonding in metal sulfoxide complexes: An update. *Coord. Chem. Rev.* **2004**, *248*, 351–375.

53. Günter, P. Holography, coherent light amplification and optical phase conjugation with photorefractive materials. *Phys. Rep.* **1982**, *93*, 199–299.

54. Yamada, A.; Tamada, H.; Saitoh, M. Photorefractive damage in $LiNbO_3$ thin-film optical waveguides grown by liquid phase epitaxy. *J. Appl. Phys.* **1994**, *76*, 1776–1783.

55. Kip, D. Photorefractive waveguides in oxide crystals: Fabrication, properties, and applications. *Appl. Phys. B* **1998**, *67*, 131–150.

56. Dieckmann, V.; Springfeld, K.; Eicke, S.; Imlau, M.; Rack, J.J. Thermal stability, photochromic sensitivity and optical properties of $[Ru(bpy)_2(OSOR)]^+$ compounds with R = Bn, BnCl, BnMe. *Opt. Express* **2010**, *18*, 23495–23503.

57. Schaniel, D.; Woike, T.; Kushch, L.; Yagubskii, E. Photoinduced nitrosyl linkage isomers in complexes based on the photochromic cation $[RuNO(NH_3)_5]^{3+}$ with the paramagnetic anion $[Cr(CN)_6]^{3-}$ and the diamagnetic anions $[Co(CN)_6]^{3-}$ and $[ZrF_6]^{2-}$. *Chem. Phys.* **2007**, *340*, 211–216.

58. Schaniel, D.; Cormary, B.; Malfant, I.; Valade, L.; Woike, T.; Delley, B.; Krämer, K.W.; Güdel, H.U. Photogeneration of two metastable NO linkage isomers with high populations of up to 76% in trans-$[RuCl(py)_4(NO)][PF_6]_2 \cdot \frac{1}{2}H_2O$. *Phys. Chem. Chem. Phys.* **2007**, *9*, 3717–3724.

59. Schaniel, D.; Woike, T.; Delley, B.; Biner, D.; Krämer, K.W.; Güdel, H.U. Generation of one light-induced metastable nitrosyl linkage isomer in $[Pt(NH_3)_4Cl(NO)]Cl_2$ in the red spectral range. *Phys. Chem. Chem. Phys.* **2007**, *9*, 5149–5157.

60. Rachford, A.A.; Petersen, J.L.; Rack, J.J. Efficient energy conversion in photochromic ruthenium DMSO complexes. *Inorg. Chem.* **2006**, *45*, 5953–5960.

61. Grusenmeyer, T.A.; McClure, B.A.; Ziegler, C.J.; Rack, J.J. Solvent effects on isomerization in a ruthenium sulfoxide complex. *Inorg. Chem.* **2010**, *49*, 4466–4470.

62. Rachford, A.A.; Petersen, J.L.; Rack, J.J. Designing molecular bistability in ruthenium dimethyl sulfoxide complexes. *Inorg. Chem.* **2005**, *44*, 8065–8075.

63. Taffa, D.H.; Kathiresan, M.; Walder, L. Tuning the hydrophilic, hydrophobic, and ion exchange properties of mesoporous TiO_2. *Langmuir* **2009**, *25*, 5371–5379.

64. Möller, M.T.; Asaftei, S.; Corr, D.; Ryan, M.; Walder, L. Switchable electrochromic images based an a combined top-down bottom-up approach. *Adv. Mater.* **2004**, *16*, 1558–1562.

65. Imlau, M.; Fally, M.; Burr, G.W.; Sincerbox, G.T. Holography and data storage. In *Handbook of Lasers and Optics*, 2nd ed.; Träger, F., Ed.; Springer-Verlag: Berlin, Germany, 2011.

66. Ostrovsky, Y.I.; Butusov, M.M.; Ostrovskaya, G.V. *Interferometry by Holography*; Springer Verlag: Berlin, Germany, 1980.

67. Vest, C.M. *Holographic Interferometry*; Wiley Interscience: New York, NY, USA, 1979.

68. Wernicke, G.; Osten, W. *Holographische Interferometrie*; Physik-Verlag: Weinheim, Germany, 1982.

69. Kreis, T. *Holographic Interferometry*; Akademie Verlag: Berlin, Germany, 1996.